Single and Multiple Binding of β-Cyclodextrin and Polymeric β-Cyclodextrins to Luminescent Ruthenium(II) α-Diimine Complexes

Wenying Xu,[†] Ajay Jain,[†] Bryan A. Betts,[†] J. N. Demas,*[,†] and B. A. DeGraff*[,‡]

Departments of Chemistry, University of Virginia, Charlottesville, Virginia 22901, and James Madison University, Harrisonburg, Virginia 22807

Received: April 27, 2001; In Final Form: September 10, 2001

A comprehensive study of the binding interactions between ruthenium complexes with multiple binding sites and monomeric and polymeric β-cyclodextrins is presented. A variety of different binding modes involving single and multiple binding arrangements are found. Binding is critically dependent on the geometry of the guest and host and hydrophobicity effects. There is an optimal spacing of the cyclodextrin units in order to exploit the geometry of the multiple attachment points of the guest. On CD binding, the complexes are shielded from oxygen quenching. Quenching can be reduced by from 3 to greater than 10 times compared to the free complex even though only a small portion of the surface of the complex is protected. The greatly enhanced shielding can be attributed to the excitation being localized in the protected region. With the polymeric hosts, the associated linker can also assist in shielding. Implications of these results to polymer supported quenchometric oxygen sensors are discussed.

Introduction

The interaction of metal complexes with microheterogeneous materials, polymers, biopolymers, etc., is an active area of interest. Cyclodextrins (CD) is a class of materials that binds a variety of substrates and mimics binding sites in biological systems.[1] There is a vast body of work on alteration of luminescence by formation of CD inclusion complexes, although most of it has been done with organic guests. Understanding the interactions of CDs and polymeric CDs has potential application in drug transport systems,[2] clean up of pollutants,[3] chemical sensing,[4] and separations.[5] There have been CD ligands and metal complexes incorporating CDs as attachments to metal complexes to provide environmental sensitivity.[6] Metal complexes, because of their variable structures and the large environmental sensitivity of their luminescence, make ideal probes for examining the binding interactions of CDs and polymeric CD hosts.[7] Also, understanding the interactions of the complexes with the hydrophobic environments characteristic of CDs will aid in the design of metal complexes for use as molecular probes and sensors.[8]

We have examined binding of both CD and polymeric CDs with pyrene and have found a number of interesting binding motifs and variations of binding strengths with CD structure.[9] As a result, we were interested in how metal complexes with multiple binding sites and multibinding site hosts can associate with each other. In particular, we were trying to sort out the different types of bindings possible, the conformational constraints on these bindings, and the role of regional hydrophobicity in controlling these interactions. We were also interested in establishing the dynamics of formation and dissociation or exchange of the different forms between each other. In this paper, we demonstrate that there are a variety of binding modes available, and many of these are unique to the polymer/multibinding site metal complex systems. The wide variety of binding modes give rise to rich photophysical responses.

* To whom correspondence should be addressed.
[†] University of Virginia.
[‡] James Madison University.

Experimental Section

Metal Complexes. All of the complexes examined were homo- and heterochelated Ru(II) complexes. These complexes are listed in Table 1 along with the abbreviations used in the paper. These complexes represent a wide range in the number and positioning of the binding sites. The metal complexes were either available from previous studies or were synthesized by standard techniques.[9] Purity was judged by the presence of only a single spot with at least one TLC system, and all complexes exhibited a single-exponential decay in a pure solvent.

Cyclodextrins. The structures of the polymeric β-cyclodextrins, also available from earlier work,[9] are shown below.

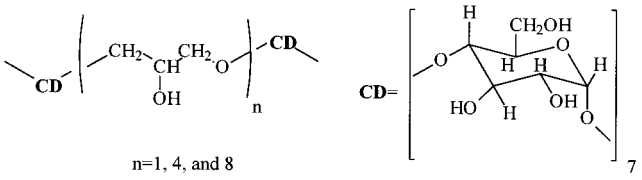

where CD is β-cyclodextrin. The linking agent was epichlorohydrin, which gives chains of $CH_2CH(OH)CH_2O$ units connecting the CDs. The polymers are abbreviated E1 ($n = 1$), E4 ($n = 4$), and E8 ($n = 8$), where the digit corresponds to the average number of linking monomer subunits connecting the CDs. Size exclusion membranes were used to ensure a minimum molecular weight of 3500. These polymers are certainly heterogeneous with respect to the number of linking subunits in each chain and the number of CDs per polymer chain.

Absorption and Emission Measurements. Absorption spectra were measured using a Hewlett-Packard 8452A Diode Array Spectrophotometer. Room-temperature fluorescence spectra were taken on a Spex Fluorolog 2+2 Spectrofluorometer using visible excitation. Emission spectra were corrected for polymer background. Oxygen-quenching studies were carried out by bubbling nitrogen, air, or oxygen through the samples.

Room-temperature lifetimes, τ's, were measured using a pulsed N_2 laser (337 nm) decay system.[10] A Tektronix TDS-540 digital oscilloscope with 1 G sample/s 8 bit digitizer was

10.1021/jp0116149 CCC: $22.00
Published on Web 12/14/2001

TABLE 1: Excited State Lifetimes of Ruthenium(II) Complexes in Water

complex	lifetime (ns)[a,b]		
	nitrogen	air	oxygen
$[Ru(phen)_3]^{2+}$	1320	503	168
$[Ru(4,7\text{-}Me_2phen)(phen)_2]^{2+}$	2020	595	141
$[Ru(5\text{-}Phphen)(phen)_2]^{2+}$	1430	546	167
$[Ru(5\text{-}Phphen)_2(phen)]^{2+}$	1740	583	170
$[Ru(5\text{-}Phphen)_3]^{2+}$	2030	560	182
$[Ru(4,7\text{-}Ph_2phen)(phen)_2]^{2+}$	3320	760	231
$[Ru(4,7\text{-}Ph_2phen)_3]^{2+}$	3550	780	212

[a] Solutions are purged with pure nitrogen, air, or oxygen. [b] Abbreviations used: phen = 1,10-phenanthroline, 4,7-Me2phen = 4,7-dimethyl-1,10-phenanthroline, 5-Phphen = 5-phenyl-1,10-phenanthroline, and 4,7-Ph_2phen = 4,7-diphenyl-1,10-phenanthroline.

used for all measurements. Signal averaging (400 transients) was used to collect each transient and data were transferred in the high resolution 16 bit mode to a computer for reduction. The emissions were monitored at the emission maxima of 600−620 nm. All complexes in pure water gave single exponential decays regardless of whether the solutions were purged with nitrogen, air, or oxygen (Table 1). In the presence of CDs, single and multiexponential luminescence decay curves were observed for different samples. Initially, individual decays were fit by nonlinear least squares to the sum of up to 3 exponentials (eq 1) using a Marquardt algorithm.[11,12] $D(t)$ is the luminescence intensity at time t, and the K's and τ's are the preexponential weighting factors and the excited-state τ's, respectively

$$D(t) = \sum_{i=1}^{3} K_i \exp(-t/\tau_i) \tag{1}$$

This information was used in the more general fitting described later. In the absence of oxygen, the lifetimes were negligibly affected by CD. Single-exponential lifetimes are precise to about 1%. We estimate that the multiexponential decay times are accurate to better than 10%.

Data Fitting. There are essentially two dynamic processes involved in our systems. There are the excited state decays of the different species, and in addition, there are the rates of equilibration between the different bound and unbound forms. Static or slow exchange modeling as well as dynamic kinetic models were used to fit the data. In static modeling, it was assumed that all excited-state decay rate constants were fast with respect to exchange between the different chemical forms. In dynamic modeling, all rate constants in the appropriate kinetic equations were used to fit the data including exchange processes.

In such complicated systems, fitting each of the individual decay curves (eq 1) to a multiexponential decay with free floating lifetimes and then trying to reconcile the different parameters from the fits at different CD concentration was an unsatisfactory approach. Parameters for the different conditions could vary too wildly, especially on minor components, to allow extracting meaningful parameters for the full kinetic scheme. For example, if a lifetime component contributes only slightly to a decay, the best fit lifetime could be grossly different from the actual lifetime. To avoid this problem, we used a global fit where parameters that should be common to all measurements were fit globally to all experiments.

All global data fitting was done by nonlinear least squares using a simplex algorithm.[11] Initially, data sets of several decay curves, each taken at a different CD concentration, were fit globally as a set with the overall error (i.e., the unweighted χ^2 or sum of the squares of the residuals for all data sets) minimized. This procedure presented two problems: the noise level on our luminescence decay curves was erratic between different samples, and different numbers of data points were used in each data fit. If one were to fit the data by just minimizing the χ^2 for all data, undue weight would be given to sets with the most points or the noisiest data. To circumvent these problems, the following procedure was used. We first obtained the best fit for each decay curve using an unconstrained single, double, or triple exponential decay (eq 1) until no improvement in the fit was observed. Since the best fits all gave randomly distributed residuals, the chi square for these fits represented the best χ^2 that could be obtained for each decay curve. In other words, these χ^2's were representative of perfect data fits. We denote these best values by $\chi_{j\text{Best}}^2$ ($j = 1...N$ for the N decay curves used in a global fit). A perfect fit to a model should have an approximate reduced chi square ($\chi_{j\text{Best}}^2$) of about 1.0.

In our global modeling, the sum of the reduced chi squares for all the decay curves was minimized:

$$\chi_r^{\,2} = (1/N)\sum_{j=1}^{N}\{(\chi_j^{\,2}\}/\{\chi_{j\text{Best}}^{\,2}\}) \tag{2}$$

where χ_j^2 is the chi square calculated for the j-th sample with the current parameters. If we had a perfect fit to all the decay curves, we would have a reduced chi square of 1. In practice, fits of 1.1−1.2 were very good overall fits and agree very well with the experimental data as judged by visual examination of the residuals plots, while values above 1.5 showed significant visual deviations.

In the global fits, some parameters must be common to all the decay curves in a titration taken at different CD concentrations. The common parameters were the rate constants, the equilibrium constants, and the static lifetimes. On the other hand, the preexponential factors were decay curve specific. While not a perfect approach for compensation for variations in the different decays curves, this approach minimized the problem of one or a few decay curves dominating the analysis. The program used for data fitting was adapted from the simplex routine used earlier.[11] While this fitting algorithm does not allow direct estimation of uncertainties, it generally appears that binding constant deviations greater than 10−20% of the reported value would produce very noticeable deviations from the best fits. We estimate this as the uncertainties on the binding constants.

Shielding Studies. We have shown that binding of CDs to metal complex blocks the exposure of the metal complex to oxygen quenching. To quantify how CD binding shields the complex from bimolecular oxygen quenching, we define a shielding factor, SF, for each CD-bound species with the following equation:

$$\mathrm{SF} = 1 - \frac{k_2(\text{bound})}{k_2(\text{free})} = 1 - \frac{1/\tau_{\text{oxygen}}(\text{bound}) - 1/\tau_{\text{nitrogen}}(\text{bound})}{1/\tau_{\text{oxygen}}(\text{free}) - 1/\tau_{\text{nitrogen}}(\text{free})} \approx 1 - \frac{\tau_{\text{nitrogen}}(\text{free})/\tau_{\text{oxygen}}(\text{bound}) - 1}{\tau_{\text{nitrogen}}(\text{free})/\tau_{\text{oxygen}}(\text{free}) - 1} \tag{3}$$

where the k_2's are bimolecular oxygen quenching rate constants for each species either in the unassociated form (free) or in a bound (bound) configuration, the subscript denotes the purge gas, and free and bound refer to the unassociated metal complex

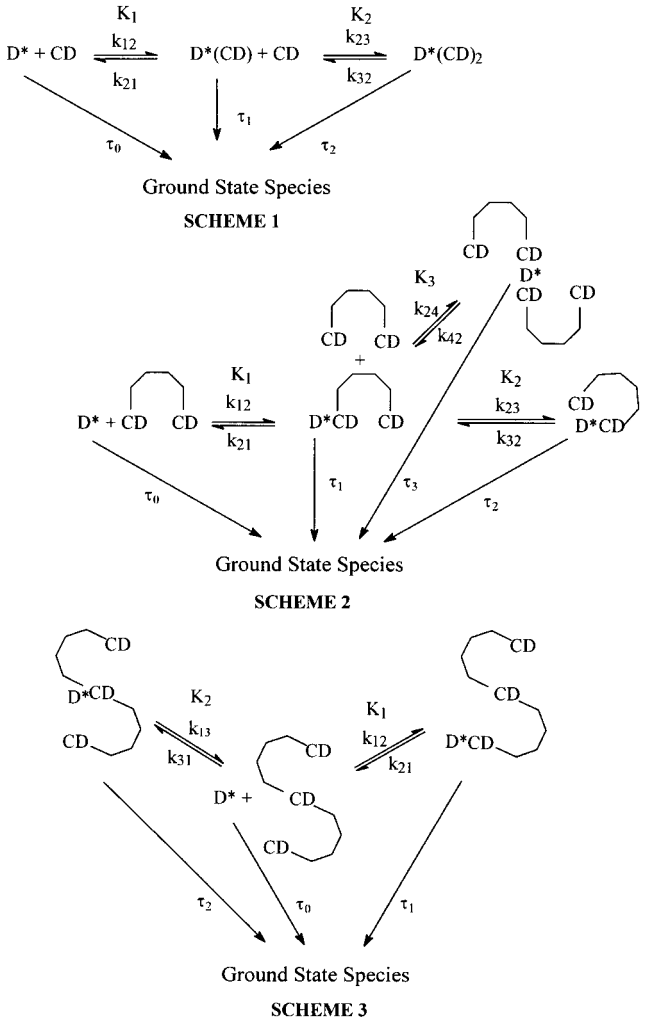

Figure 1. Different binding schemes for monomeric and polymeric CDs to mono- and di-binding site substrates.

and the different bound species, respectively. For each bound species, the lifetime is computed from the best fits for the different binding models. For different systems, there could be several forms of the association complex (e.g., singly or doubly capped) with each one treated separately. A shielding factor (SF) of 1 corresponds to no quenching of the bound form or complete shielding. A SF of 0 means no shielding of the excited state for oxygen quenching by CD binding. The approximate form (eq 3) was used here and is based on the assumption that the intrinsic excited state lifetime is unaffected by binding to CDs. This assumption is borne out by the absence of a CD effect on the lifetimes in the absence of oxygen. SFs are probably accurate to ±0.05 for the simpler systems and 0.10 for the more complex schemes.

Results and Discussion

Several types of behavior for the different systems were expected. These schemes are shown in Figure 1. With only a single binding site (i.e., the mono 5-Phphen complex), we would expect to see only a single binding with either β-CD or polymeric CDs. We might expect that the binding constants should be comparable on a CD basis for the polymeric CDs. When there are multiple binding sites on the guest, sequential binding to the available sites by monomeric CD would be expected, as shown in Scheme 1 of Figure 1.

Scheme 1 is appropriate when the guest has one or two binding sites. We show sequential binding of one and two CDs to the guest.

For polymeric hosts with guests having multiple binding sites, an alternative scheme exists if the host has multiple binding sites. If the linker between the CDs is long enough, it is possible for a second pendant CD on the polymer chain to fold back and bind to a second site on the guest after initial bimolecular binding to the first site. This is shown schematically in Scheme 2 of Figure 1 with a second intramolecular K_2. K_2 should depend critically on the length of the linker between the CDs relative to the spacing of the two binding sites. Too short a chain and double capping cannot occur, while with too long a chain the second CD is so far away from the binding site that entropic factors minimize binding. In addition, there is still the possibility of two independent polymer chains binding to a single metal complex with a bimolecular K_3. This is shown schematically in Scheme 2 as a parallel reaction path for the singly bound guest. At high enough CD concentrations this double chain binding could become significant.

Scheme 3 of Figure 1 is a variation of Scheme 1 with a single binding site. Binding at this single site arises from competition between two spectroscopically distinguishable host sites on the same polymer chain. Anticipating our results, we show a single polymer that can bind at two different positions on the polymer chain.

Within the different chemical models, we consider two kinetic cases, the slow exchange or static limit and the dynamic case. In slow exchange the concentrations of all species are determined by their initial equilibrium values, and exchange between the different forms is slow compared to the excited-state decay times of the different species. In the dynamic case, the excited-state lifetimes and the exchanges between different forms are comparable. To model this latter case requires the solution of systems of coupled differential equations.[13] In the dynamic limit of very rapid exchange compared to the excited state lifetimes, the decays all become single exponentials. This limit did not apply to any of our systems, as all of the decays in CD-containing solutions were multiexponential.

In the slow exchange limit, Scheme 2 (without a second bimolecular addition) and a single binding Scheme 1 are mathematically indistinguishable, except that the apparent K_1 of Scheme 1, denoted by K_{app}, is related to the Ks of Scheme 2 by

$$K_{app} = (K_2 + 1)K_1 \tag{4}$$

However, the two can generally be distinguished on chemical arguments or by the presence of a third lifetime in Scheme 2.

It was our hope that kinetic modeling would allow us to differentiate between these different cases and to obtain information on the structural properties controlling the strength of the interactions. In practice, we found that the rates obtained by the full kinetic analyses were so slow compared to the reciprocal lifetimes that the quality of the fit was not improved significantly by involving the extra parameters of dynamic exchange. By increasing the magnitude of k_{12}, we were able to determine that the fits deteriorated substantially with $k_{12} > 10^8$ M^{-1} s^{-1}. Therefore, all of the subsequent modeling used the slow exchange limit. We turn now to examination of the individual complexes.

Typical fits are shown in Figures 2 and 3. Figure 2 is an excellent fit for $[Ru(5\text{-Phphen})_2(phen)]^{2+}$ with CD using a sequential Scheme 1 model ($\chi_r^2 = 1.03$). Figure 3 shows a similar fit for $[Ru(Me_2phen)_3]^{2+}$ with the E8 polymer ($\chi_r^2 =$

TABLE 2: Binding and Photophysical Properties of Ruthenium Complexes with β-CD and Polymeric CDs

complex	CD	scheme	K_1	K_2	τ_1, ns	τ_2 (SF), ns	τ_3 (SF), ns	χ_r^2
$[Ru(phen)_3]2+$	CD	no binding						
$Ru(5\text{-}Phphen)(phen)_2^{2+}$	CD	1 (1:1)	0.55 mM^{-1}		174	392 (0.65)		1.19
	E1	1 (1:1)	0.63 mM^{-1}		175	494 (0.75)		1.41
	E4	3 (parallel 1:1)	0.60 mM^{-1}	0.06 mM^{-1}	171	620 (0.83)	1500 (1.00)	1.61
	E8	1 (1:1)	0.78 mM^{-1}		170	1022 (0.95)		1.26
$[Ru(5\text{-}Phphen)_2(phen)]^{2+}$	CD	1 (1:1, 1:2)	0.61 mM^{-1}	0.27 mM^{-1}	184	441 (0.68)	430 (0.67)	1.04
	E4	2 ($K_2 = 0$)	7.7 mM^{-1}	0.10 mM^{-1}	184*	705 (0.85)	1740* (1.0)	1.42
	E8	2 ($K_2 = 0$)	3.8 mM^{-1}	0.40 (intramolecular foldback)	179	873 (0.89)	1630 (0.99)	1.41
$[Ru(4,7\text{-}Ph_2phen)(phen)_2]^{2+}$	CD	1 (1:1)	1.1 mM^{-1}	0.001 mM^{-1}	220	584 (0.65)	556 (0.6)	1.07
	E4	2 ($K_3 = 0$)	1.70 mM^{-1}	0.91 (intramolecular foldback)	213	505 (0.58)	1282 (0.88)	1.17
	E8	2	1.25 mM^{-1}	0.30 (intramolecular foldback)	216	985 (0.82)	2317 (0.97)	1.31 ($\leq$1 mM)
$[Ru(4,7\text{-}Me_2phen)(phen)_2]^{2+}$	E8	2	0.032 mM^{-1}	0.27 (intramolecular foldback)	140	547 (0.80)	1870* (1.0)	1.20

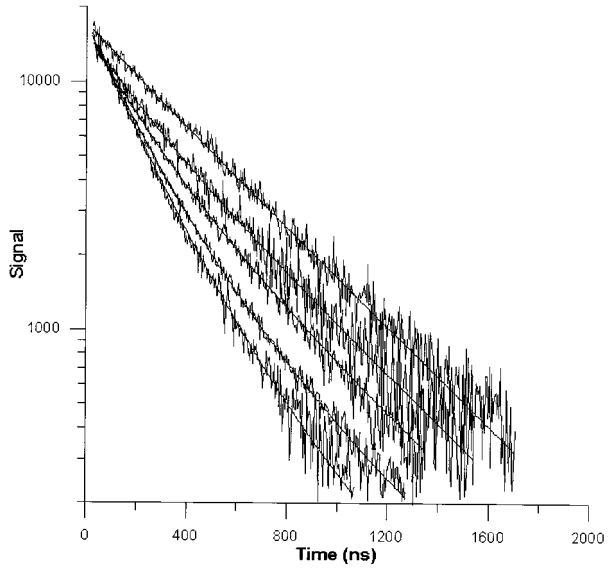

Figure 2. Luminescence titration of $[Ru(Phphen)_2(phen)]^{2+}$ with CD. Seven data decays with concentrations ranging from 0.1 to 6 mM were used. Only five representative decays are shown to improve viewing. The solid lines are for the Scheme 1 model with two step sequential bimolecular bindings ($\chi_r^2 = 1.03$).

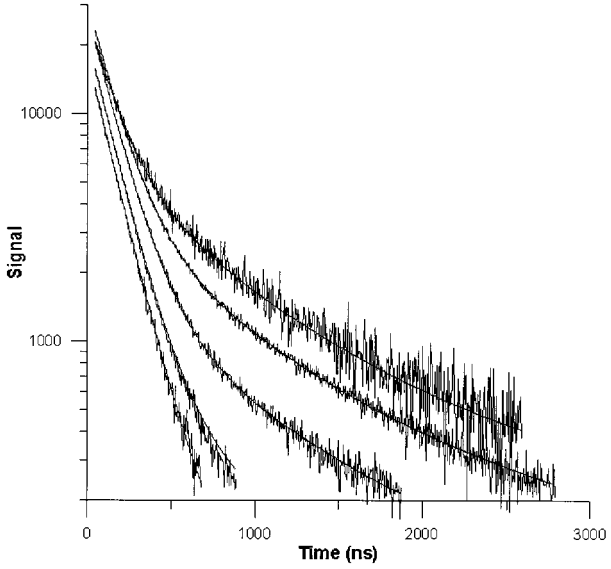

Figure 3. Luminescence titration of $[Ru(Me_2phen)_3]^{2+}$ with the 8E polymer. Seven data decays with concentrations ranging from 0.05 to 8 mM were used. Only five representative decays are shown to improve viewing. The solid lines are a Scheme 2 fit with bimolecular addition followed by intramolecular foldback ($\chi_r^2 = 1.20$).

1.20). We turn now to specific systems and the justification for the schemes of Figure 1. The results of the fitting schemes are summarized in Table 2.

$[Ru(phen)_3]^{2+}$. As a control, it was verified that there was no evidence for CD binding to the unsubstituted 1,10-phenanthroline portion of the complexes. The lifetime of $[Ru(phen)_3]^{2+}$ in pure water and in 6 mM CD was examined in both deoxygenated and oxygenated media. In deoxygenated water, the lifetimes were 1320 and 1324 ns with and without CD, respectively. In oxygen saturated water, the lifetimes were within experimental error of each other, 167 and 174 ns without and with CD, respectively. If CD were associated, it should perturb the excited-state lifetime or shield the complex from oxygen quenching. Neither is observed. So there is no evidence for significant CD binding to an unsubstituted phen under our measurement conditions.

While CD binding to phen has been observed for $Re(phen)(CO)_3NCR^+$ species,[14] the phen in these cases has far less geometric shielding from the CD than in the Ru(II) trischelated complexes. Therefore, the current Ru(II) data is not incompatible with the Re(I) data.

$Ru(5\text{-}Phphen)(phen)_2^{2+}$. $Ru(5\text{-}Phphen)(phen)_2^{2+}$ is the simplest complex in the series for which we would expect CD binding. It should ideally present only one binding site for formation of CD inclusion complexes. This suggestion is correct. With CD, this system is fit quantitatively by Scheme 1 with only a single binding constant ($K_2 = 0$). The binding constant is about 0.6 mM^{-1} and is comparable to that found earlier for this complex using far less sensitive equipment.[15] It is also similar to binding constants of phenyl derivatives with α-CD. There is significant shielding of the excited state to oxygen quenching (SF = 0.65) by the bound CD as shown by the increase in shielded lifetime.

We turn now to the polymeric CDs with this complex. The E1 and E8 polymers are quite similar to β-CD and show only a simple 1:1 binding. The polymer bound lifetime is much longer than the bound lifetime in the CD system. This is consistent with a greater degree of steric shielding of the complex by the

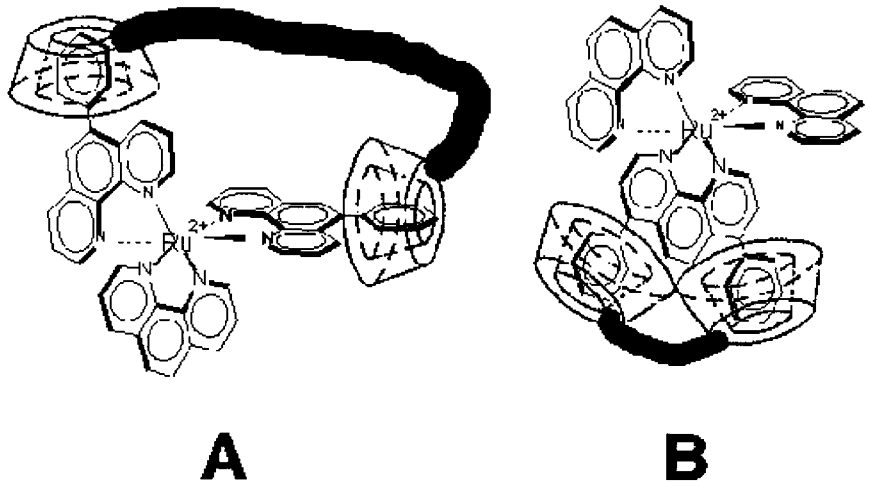

Figure 4. Schematic representation of the binding of multiple CDs to $[Ru(5\text{-}Phphen)_2(phen)]^{2+}$ and $[Ru(Ph_2phen)\ (phen)_2]^{2+}$ to CDs or polymeric CDs. The solid heavy line represents the variable length polymer linking the CDs. For monomeric CDs, there would be no linker. Clearly, the polymer length is critical in adjusting the position of linked CDs to the separation of the phenyl groups.

bulky polymer. The shielding becomes more pronounced as the bulk of the polymer increases, which is physically reasonable.

The E4 polymer presents a more interesting scenario. Unlike the other two polymers, it is not fit by Scheme 1 even with the addition of a second bimolecular step. The best fit is by either Scheme 3 with a parallel 1:1 model or the equivalent Scheme 2 with $K_2K_3 = 0$ (i.e., only a second intramolecular binding). Scheme 2 makes no chemical sense. First, it is difficult to envision a second binding site on this complex. Further, if there were a second binding site accessible for intramolecular binding to the E4 polymer, we would expect the E8 polymer to behave similarly. However, the E8 polymer shows only 1:1 binding with no evidence of this double intramolecular binding. We conclude that Scheme 3 is the most appropriate for the E4 polymer.

If Scheme 3 is the correct one, we must have a plausible explanation for the parallel binding and the differences in properties. On the average, the E4 polymer contains only 3−4 CDs per polymer chain. There are two types of binding possible. Binding to the complex can be either via terminal CDs or interior CDs. With the relatively short linker, we would expect there to be differences between terminal and interior binding as far as association of the CDs with the complex. We envision that the two binding modes will cause differences in shielding of the excited state. Terminal binding would allow shielding from one side of the polymer chain, while interior binding would allow wrap-around shielding from both sides.

In our fitting, the longest lifetime and the lowest binding constant are coupled. In the framework of our model, this would correspond to binding to the interior CDs. We attribute the lower binding constant for the interior CDs to two factors. On the average, there are fewer interior CDs than terminal ones. Second, the interior CDs are less accessible for binding than the terminal ones.

The reason the E8 polymer does not show this effect is that the linker is much longer. Nearest-neighbor effects are minimized, and it does not matter whether binding is interior or terminal.

$[Ru(4,7\text{-}Me_2phen)(phen)_2]^{2+}$. As a test of the degree of hydrophobicity required to give CD inclusion complexes, we examined $[Ru(4,7\text{-}Me_2phen)(phen)_2]^{2+}$ with the E8 polymer. The methyls represented a somewhat hydrophobic substituent and our other results suggested that the E8 polymer was the most aggressive binder. This system was best fit with Scheme 2 with no second bimolecular step. This is reasonable since the complex has two binding sites (the methyls), and the polymeric CD is set up for double binding. The best fit parameters, however, show that the binding is very weak (at least a factor of 10) compared to the phenyl substituted cases, as would be expected on the basis of the relative hydrophobicity of a methyl versus a phenyl and the superior match of the phenyl group to the CD cavity compared to the smaller methyl.

$[Ru(5\text{-}Phphen)_2(phen)]^{2+}$. We turn now to this more complex system, which has two sterically far removed CD binding sites. This is shown schematically in Figure 4A, where monomeric CDs would not have the interconnecting polymer. These sites are sufficiently distant that they should behave largely independently.

This is validated by the observed behavior with monomeric CD, which is fit by Scheme 1 with sequential binding. Two distinct binding constants are observed in about a two-to-one ratio, which is consistent with the absence of steric interaction. Also, the first binding constant is comparable to that observed for $Ru(5\text{-}Phphen)(phen)_2^{2+}$ with CD.

The most interesting aspect of CD binding is that, although the first CD greatly shields the complex, the second binding has little additional shielding effect. This behavior can be rationalized on the basis of localized excitation. The emission red shifts on both mono and bis 5-Phphen complexes on addition of CD. This lowering of the excited state energy corresponds to a reduction of the energy of the MCLT excitation on the 5-Phphen ligand. If the excitation is localized in one of the protected ligands, then the degree of shielding will be largely unaffected by double capping since the two ligands are spatially so separated.

The E4 and E8 polymers are fit by Scheme 2 with only an intramolecular second binding ($K_3 = 0$). The first thing one notices is the much larger K_1's for these polymers than for CD itself. Clearly, the polymer chain is enhancing the binding to these bis complexes while having no effect on the mono complex. This must be associated with the polymer chains finding a favorable interaction with the second uncapped phenyl. We envision entanglement of the chains with the protruding second phenyl.

The intramolecular binding constant increases significantly on going from E4 to E8. Space filling models indicate that the E4 linker is just barely long enough to permit double capping. The E8 is more than long enough to permit double capping, but not so long as to keep the adjacent CDs entropically away from the binding partner. Thus, the superior intramolecular binding of E8 versus E4. This is analogous to the chelate effect in inorganic complexes.

The very high degree of shielding of the double capped intramolecular foldback complex suggests that the linkage plays a vital role in shielding the complex from oxygen quenching. Since both ends of the polymer linker are anchored on the complex, the polymer fills in the regions between the two ligands and protects the excited ligand from incoming oxygen. Monomeric CD leaves a big cleft for entry of oxygen and, thus, does not give the strong shielding.

Note that even the single capped complex with E8 and E4 shows considerably greater shielding than the mono complex. This is again consistent with the association of the polymer chains with the complexes.

$[Ru(4,7\text{-}Ph_2phen)(phen)_2]^{2+}$. For monomeric CD, K_1 is roughly a factor of 2 larger than for $[Ru(5\text{-}Phphen)(phen)_2]^{2+}$. K_2 is unmeasurably small. Molecular models suggest that binding of a second CD will be much less favorable because of steric hindrance from the first binding (Figure 4A). It is also possible that this small apparent second binding is to some degree a fitting artifact. If the best fit lifetimes between the singly and doubly capped forms are very similar, this could reduce our ability to resolve the second component. However, it seems clear that K_2 is much smaller than that for the other double phenyl-containing complex, $Ru(5\text{-}Phphen)_2phen$.

The E4 results are best fit by Scheme 2 with $K_3 = 0$. The intramolecular binding constant is rather large (0.9) and significantly higher than that for $Ru(5\text{-}Phphen)_2phen$. This is consistent with the molecular geometry (Figure 4B). The Ph_2-phen complex requires only a short polymer spacer to place the CD into optimal position for binding to the second phenyl, while the $Ru(Phphen)_2phen$ (Figure 4A) requires a four-linker element at a minimum.

For the E8 polymer up to 1 mM, Scheme 2 fits best with K_1 of 0.3. K_1 for E8 drops by about a factor of 3 compared to E4. We attribute this to the entropic effect of moving the second CD farther from the second binding site. This result is the opposite of $[Ru(Phphen)_2phen]^{2+}$, where K_2 increases by about a factor of 4 on going from E4 to E8, which is the expected direction because unlike the E8 the E4 polymer linker is not long enough to reach easily to the second binding site.

At higher concentrations of E8, we must add the bimolecular path K_3 for good fits. Even with global fitting, however, we do not feel that we can extract reliable parameters from this rather complicated system. However, the ability to satisfactorily mimic the data suggests that the more complicated model is appropriate.

Relevance to Polymer Supported Sensors. Polymer-supported luminescent molecules are widely used as oxygen sensors.[7] It is well-known that Stern−Volmer quenching plots of such systems are generally concave downward. This curvature has been attributed to heterogeneity of the sensing molecules in the support with different quenching properties. Our results with different CDs clearly demonstrates that quenching properties are highly dependent on the organization of polymers around the complex and that relatively small changes in the binding can produce large differences in the quenching. Since the metal complexes dissolved in polymers are certainly in less organized structures, these results further support the heterogeneity model as the source of the nonlinear Stern−Volmer quenching plots. Similar sorts of heterogeneity have been observed in polymer supported metal ion sensors.[16]

Conclusions

Our results demonstrate how to design metal complex guest−host systems with optimal binding. Critical to binding is optimal overlap of as many different binding sites as possible with the host. This can only be achieved if the guest and host sites are spaced appropriately to permit binding. Methyl groups are orders of magnitude poorer than phenyls for binding to CDs. While the first binding constant of polymeric systems is similar to that for the monomeric systems, the additional intramolecular binding of polymeric systems can shift the equilibrium far toward complex formation by reducing the concentration of the first binding product.

In terms of effects on excited state properties, both polymeric and monomeric CDs have a large effect on shielding of the excited states from oxygen quenching. This results in multiexponential decays. The polymeric systems can be much more effective at oxygen shielding than the monomeric systems. This is presumably due to the linking polymer being dragged along with the binding groups, which fills in the voids around the metal complex and impedes entrance of oxygen.

Nonexponential decays with and without oxygen quenching (i.e., nonlinear Stern−Volmer quenching plots) are observed for metal complex molecular probes and sensors dispersed in polymers. This result has been attributed to heterogeneous binding sites and differential oxygen quenching between the different binding sites.[15] The current results show that heterogeneity in oxygen quenching can result even in homogeneous systems, which is a result that adds further support to binding site heterogeneity as being the source for the widely observed nonlinear Stern−Volmer quenching plots for quenchometric oxygen sensors.

Acknowledgment. We thank the National Science Foundation for support through Grants CHE 97-26999 and CHE 00-94777. We also acknowledge support from The Petroleum Research Fund (Grant #29550-B3).

References and Notes

(1) Szejtli, J. *Chem. Rev.* **1998**, *98*, 1743−1753. (b) Hoskin, F. C. G.; Steeves, D. M.; Walker, J. E. *Biol. Bull.* **1999**, *197, 2*, 284−285.

(2) (a): Li. P.; Zhao, L. W.; Yalkowsky, S. H. *J. Pharm. Sci.* **1999**, *88*, 1107−1111. (b) Uekama, K.; Hirayama, F.; Irie, T. *Chem. Rev.* **1998**, *98*, 2045−2076.

(3) (a) Tanada, S.; Nakamura, T.; Kawasaki, N.; Torii, Y.; Kitayama, S. *J. Colloid Interface Sci.* **1999**, *217*, 417−419. (b) Mccray, J. E.; Brusseau, M. L. *Environ. Sci. Technol.* **1999**, 33, 89−95. (c) Brusseau, M. L.; Wang-, X. J.; Wang, W. Z. *Environ. Sci. Technol.* **1997**, *31*, 1087−1092. (d) Bizzigotti, G. O.; Reynolds, D. A.;- Kueper, B. H. *Envion. Sci. Technol.* **1997**, *31*, 472−478.

(4) (a) Liu, Y.; Chen, Y.; Li, B.; Wada, T.; Inoue, Y. *Chem.—Eur. J.* **2001**, *7*, 2528−2535. (b) Tanabe, T.; Touma, K.; Hamasaki, K.; Ueno, A. *Anal. Chem.* **2001**, *73*, 3126−3130.

(5) (a) Hamai, S.; Sakurai, H. *Anal. Chim. Acta* **1999**, *402*, 53−58. (b) Koide, T.; Ueno, K. *Anal. Sci*. **1999**, *15*, 791−794. (c) Ma, L. Y.; Han, J. H.; Wang, H.; Gu-J. L.; Fu, R. N. *Electrophoresis* **1999**, *20*, 1900−1903. (d) Alcock, N. W., Barker, P. R.; Haider, J. M.; Hannon, M. J.; Painting, C. L.; Pikramenou, Z.; Plummer, E. A.; Rissanen, K.; Saarenketo, P. J. *Chem. Soc., Dalton Trans.* **2000**, *9*, 1447−1461 2000. (e) Robertson, A.; Shinkai, S. *Coord. Chem. Rev.* **2000**, *205*, 157−199.

(6) (a) Brügger, N.; Deschenauz, R.; Ruch T.; Ziessal, R. *Tetrahedral Lett.* **1992**, *27*, 3871−3874. (b) Deschenauz, R.; Ruch T.; Deschenauz, P.-F.; Juris, A.; Ziessal, R *Helv. Chimi. Acta* **1995**, *78*, 619−628. (c) Venema, F.; Rowan, A. E.; Nolte, R. J. M. *J. Am. Chem. Soc. 118*, 257−258. (d) Weidner, S.; Pikranenou, Z. *Chem. Commun.* **1998**, 1473−1474.

(7) (a) Lakowicz, J. R. *Principles of Fluorescence Spectroscopy*, 2nd ed.; Kluwer Academic/Plenum Publishers: New York, 1999. (b) Balzani, V.; Juris, A. *Coord. Chem. Rev*. **2001**, *211*, 97−115. (c) Demas, J. N.; DeGraff, B. A. *Coord. Chem. Rev*. **2001**, *211*, 317−351.

(8) (a) Hartmann, P.; Trettnak, W. *Anal. Chem.* **1996**, *68*, 2615−2620. (b) Mills, A. *Analyst* **1999**, *124*, 1301−1307 and 1309−1314. (c) Mills, A.; Thomas, M. D. *Analyst*, *1998*, 1135−1140. (d) Xu, WY.; McDonough, R. C., III; Langsdorf, B.; Demas, J. N.; DeGraff, B. A. *Anal. Chem*. **1994**, *66*, 4133−41.

(9) Xu, WY.; Demas, J. N.; DeGraff, B. A.; Whaley, M. *J. Phys. Chem.* **1993**, *97*, 6546−6554.

(10) Leasure, R. M.; Sacksteder, L.; Nesselrodt, D.; Demas, J. N.; DeGraff, B. A. *Inorg. Chem.* **1991**, *30*, 3722.

(11) Demas, J. N.; Demas, S. E. *Interfacing and Scientific Computing on Personal Computers*; Allyn & Bacon: New York, 1990.

(12) Demas, J. N. *Excited-State Lifetime Measurements*; Academic Press: New York, 1983.

(13) Berberan-Santos, M. N.; Martinho, J. M. G. *J. Chem. Educ*. **1990**, *67*, 375−379.)

(14) Sacksteder, L.; Lee, M.; Demas, J. N.; DeGraff, B. A., *J. Am. Chem. Soc.* **1993**, *115*, 8230−8238.

(15) Cline, III, J. I.; Dressick, W. J.; Demas, J. N. DeGraff, B. A. *J. Phys. Chem*. **1985**, *84*, 94−7.

(16) Rowe, H.; Xu, WY.; Demas, J. N.; DeGraff, B. A. *Appl. Spectosc*., in press.